https://doi.org/10.5194/amt-2022-179
Preprint. Discussion started: 27 June 2022

Atmospheric Measurement Techniques Discussions

Reducing errors on estimates of the carbon uptake period based on time series of atmospheric CO_2

Theertha Kariyathan[1,2], Wouter Peters[2], Julia Marshall[3], Ana Bastos[1], Pieter Tans[4], and Markus Reichstein[1]

[1]Max Planck Institute for Biogeochemistry
[2]Wageningen University and Research
[3]Deutsches Zentrum für Luft- und Raumfahrt (DLR), Institut für Physik der Atmosphäre, Oberpfaffenhofen, Germany
[4]Climate Monitoring Laboratory, National Oceanic and Atmospheric Administration, 325 Broadway, Boulder, CO80305, USA

Correspondence: Theertha Kariyathan (tkariya@bgc-jena.mpg.de)

Abstract. Long, high-quality time series measurements of atmospheric greenhouse gases show interannual variability in the measured seasonal cycles. These changes can be analyzed to better understand the carbon cycle and the impact of climate drivers. However, nearly all discrete measurement records contain gaps and have noise due to the influence of local fluxes or synoptic variability. To facilitate analysis, filtering and curve-fitting techniques are often applied to these time series. Previous studies have recognized that there is an inherent uncertainty associated with this curve fitting and the choice of a given mathematical method might introduce biases. Since uncertainties are seldom propagated to the metrics under study, this can lead to misinterpretation of the signal. In this study, we present a novel curve fitting method and an ensemble-based approach that allows the uncertainty of the metrics to be quantified. We apply it here to Northern Hemisphere CO_2 dry air mole fraction time series. We use this ensemble-based approach to analyze different seasonal cycle metrics, namely the onset, termination, and duration of the carbon uptake period (CUP), i.e., the time of the year when the CO_2 uptake is greater than the CO_2 release. Previous studies have diagnosed CUP based on the dates on which the detrended, zero-centered seasonal cycle curve switches from positive to negative (the downward zero-crossing date) and vice versa (upward zero-crossing date). However, we find that the upward zero-crossing date is sensitive to the skewness of the CO_2 seasonal cycle during the net carbon release period. Hence, we propose an alternative method to estimate the onset and termination of the CUP based on a threshold defined in terms of the first-derivative of the CO_2 seasonal cycle (First-derivative threshold (FDT) method). Further, using the ensemble-based approach and an additional curve fitting algorithm, we show that (a) the uncertainty of the studied metrics is smaller using the FDT method than when estimated using the timing of the zero-crossing dates, and (b) the onset and termination dates derived with the FDT-method provide more robust results, irrespective of the curve-fitting method applied to the data. The code is made freely available under a Creative Commons-BY license, along with the documentation in this paper.

https://doi.org/10.5194/amt-2022-179
Preprint. Discussion started: 27 June 2022

Atmospheric Measurement Techniques Discussions

1 Introduction

Ongoing measurements of the atmospheric CO_2 mixing ratio at Mauna Loa (MLO), initiated by Charles D. Keeling in 1958, have revealed an increase in CO_2 mole fraction in the atmosphere. Increase in atmospheric CO_2 due to release of carbon from fossil fuel burning and land-use change is buffered by the ocean and land biosphere CO_2 uptake (Keeling, 1960). Since then, many studies have used high precision measurements of greenhouse gases at MLO and other sites across the globe to better understand the role of CO_2 in global climate (e.g. Langenfelds et al., 2002; Keeling et al., 2017; Barlow et al., 2016). The analysis of such long, high-quality atmospheric time series helps to identify and isolate the long-term trends, inter-annual variability and seasonality of climatically important greenhouse gases (Thoning et al., 1989). However, these measurement records contain gaps and are influenced by local fluxes or synoptic scale variability, which induce noise on the underlying climate signals. Hence the use of filtering and curve-fitting techniques to obtain smooth and continuous data has been an inevitable part of such studies (Trivett et al., 1989). The choice of mathematical method for data processing can, however introduce biases that can result in misinterpretation of the signal (Nakazawa et al., 1997; Tans et al., 1989; Pickers and Manning, 2015).

Curve-fitting methods are often used to pre-process atmospheric time series for analysis. Three examples are found in the commonly-used software packages, HPspline (Bacastow et al., 1985), CCGCRV (Thoning et al., 1989) and STL (Cleveland et al., 1990). Each of these methods produce a gap-filled time series that contains the important features of the atmospheric record, however the resultant fitted curves vary significantly from each other owing to differences in their response to gaps and outliers in the original data. Pickers and Manning (2015) addressed the sensitivity of scientific conclusions to the curve-fitting method used, by repeating a scientific study (Piao et al., 2008) using two additional curve-fitting method. Both studies looked at changes in the CO_2 seasonal cycle zero-crossing date for ten mid-to-high-latitude, Northern Hemisphere stations. The re-analysis by Pickers and Manning (2015) found that the major conclusion of Piao et al. (2008) was robust, but that inferences at individual stations depended on the curve fitting method. Thus, the impact of bias introduced by data processing methods can vary based on the data set used and the type of analyses performed. Each method has its strengths and weaknesses; hence Pickers and Manning (2015) argued that data must be analyzed with multiple approaches to ensure that results are robust and free from bias. Despite this recommendation, studies that focus on metrics of time series such as the zero-crossing dates or seasonal cycle amplitude usually use a single curve-fitting method for analysis (e.g. Park et al., 2019; Piao et al., 2018), which can lead to differences in the conclusions that are drawn. An example is the disagreement in the direction of the trend of the CO_2 seasonal cycle amplitude (SCA) at Alert, Canada between Chan and Wong (1990) and Keeling et al. (1996), as shown by Pickers and Manning (2015).

Some metrics derived from the CO_2 time series can be highly sensitive to data gaps and noise, hence approximations are used to estimate their value. One example is the timing of the carbon uptake period (CUP). The CUP is the time of year during which the CO_2 uptake is greater than the CO_2 release. The onset and termination of the CUP are marked by the spring maximum and late summer minimum of the seasonal cycle, respectively. However, the CO_2 seasonal cycle at many observational

https://doi.org/10.5194/amt-2022-179
Preprint. Discussion started: 27 June 2022

Atmospheric Measurement Techniques Discussions

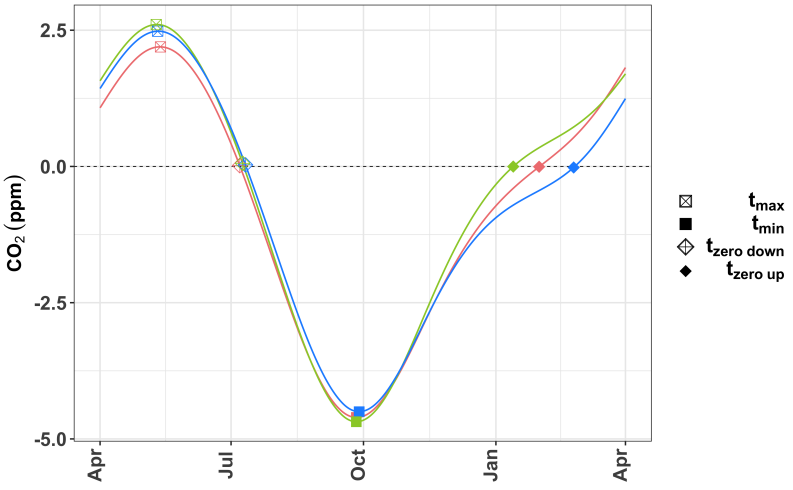

Figure 1. Diagram showing how the skewness of the seasonal cycle can influence the estimation of the CUP based on zero-crossing dates. The three seasonal cycles have similar seasonal cycle maxima, minima and downward zero-crossing dates but very different upward zero-crossing dates.

sites is characterized by a flat peak or multiple peaks in winter, making it difficult to estimate the start of the CUP by using the maximum of the seasonal cycle. To avoid this problem, previous studies have used the comparatively more unambiguous zero-crossing dates to determine the timing and duration of the CUP (e.g. Piao et al., 2008). The zero-crossing dates are the two dates in the seasonal cycle when the detrended CO_2 curve crosses the zero-line (an imaginary line passing through 0 ppm in the detrended CO_2 seasonal cycle). This approximation is based on the assumption that, if the shape of the seasonal cycle does not change significantly, a change in the phase at one point (e.g., maximum) of the seasonal cycle can be traced as a relative phase change at other points (Barichivich et al., 2012). However, this assumption breaks down if the shape of the seasonal cycle changes from year to year, and the CUP estimated using the zero-crossing dates may be erroneous. This is illustrated in Fig. 1.

In this study, we present a novel ensemble-based method to quantify the uncertainty in the CO_2 seasonal cycle metrics, arising from curve fitting data with noise and data gaps. We first use this method to show that the zero-crossing dates are not the best proxy for determining the timing and duration of the CUP when uncertainty is considered, and we propose an alternative method using a threshold defined by the first-derivative of the seasonal cycle, which we refer to as the first-derivative threshold method (FDT method). The FDT method is independent of the skewness of the seasonal cycle and it can better constrain the timing and duration of the CUP than the zero-crossing method. Next we test if the ensemble approach is sensitive to the specific curve-fitting method applied by fitting the data using the commonly-used CCGCRV method. The measurements used in this study are presented in Sect. 2 and the steps for the uncertainty estimate using an ensemble-based approach and the FDT method

https://doi.org/10.5194/amt-2022-179
Preprint. Discussion started: 27 June 2022


Atmospheric Measurement Techniques Discussions

for estimating the timing and duration of the CUP are presented in Sect. 3. The results and the discussions on the findings can be found in Sect. 4 and Sect. 5 respectively, and Sect. 6 summarizes the findings of this study.

2 Data

Table 1. Observational sites of NOAA/ESRL network used in this study

Station name	Station code	Latitude	Longitude	Time period	Data Source
Mauna Loa, Hawaii, United States	MLO	19.47°N	155.57°W	1977-2017	(Dlugokencky et al., 2019)
Assekrem, Algeria	ASK	23.26°N	5.63°E	1996-2018	(Dlugokencky et al., 2020)
Sand Island, Midway, United States	MID	28.21°N	177.36°W	1986-2018	(Dlugokencky et al., 2020)
Weizmann Institute of Science at the Arava Institute, Ketura, Israel	WIS	29.96°N	35.06°E	1996-2018	(Dlugokencky et al., 2020)
Terceira Island, Azores, Portugal	AZR	38.76°N	27.37°E	1996-2018	(Dlugokencky et al., 2020)
Niwot Ridge, Colorado, United States	NWR	40.05°N	105.58°W	1976-2018	(Dlugokencky et al., 2020)
Shemya Island, Alaska, United States	SHM	52.71°N	174.12°E	1986-2018	(Dlugokencky et al., 2020)
Barrow Atmospheric Baseline Observatory, United States	BRW	71.29°N	156.61°W	1972-2017	(Dlugokencky et al., 2019)
Ny-Alesund, Svalbard, Norway and Sweden	ZEP	78.90°N	11.88°E	1995-2018	(Dlugokencky et al., 2020)
Alert, Nunavut, Canada	ALT	82.50°N	62.50°W	1986-2017	(Dlugokencky et al., 2019)

We use discrete CO_2 dry air mole fraction from flask measurements from ten observational sites of the NOAA/ESRL network (Dlugokencky et al., 2019, 2020), ranging from 19°N to 82°N latitude. Table 1 lists the station names, station codes, their locations and the studied time period for each station (longer time records are available for MLO and NWR but these years have large data gaps of an year or more hence are not considered for analysis. At these observational sites, air is sampled in glass flasks under background conditions, hence the dry air mole fractions from the air samples are representative of the zonal mean atmospheric composition (Langenfelds et al., 2002). These air samples are collected weekly in pairs for quality control, and pairs with a difference less than 0.5 ppm between the two samples are flagged as good-quality data ("good pairs") (Dlugokencky et al., 2019, 2020). For our analysis, we use the mean value of each pair considered as "good pairs" and exclude low-quality measurements, which introduces irregular gaps in the data. The mean seasonal cycle of the higher latitude stations (above 45°N latitude, i.e. SHM, BRW, ZEP, and ALT) is characterized by a broader maxima or multiple peaks in winter. Some lower latitude stations like MLO, MID and NWR have distinct seasonal cycles with clearly defined maxima, while others, like ASK, AZR and WIS, have broader peaks. (Fig. 2).

https://doi.org/10.5194/amt-2022-179
Preprint. Discussion started: 27 June 2022

Atmospheric Measurement Techniques Discussions

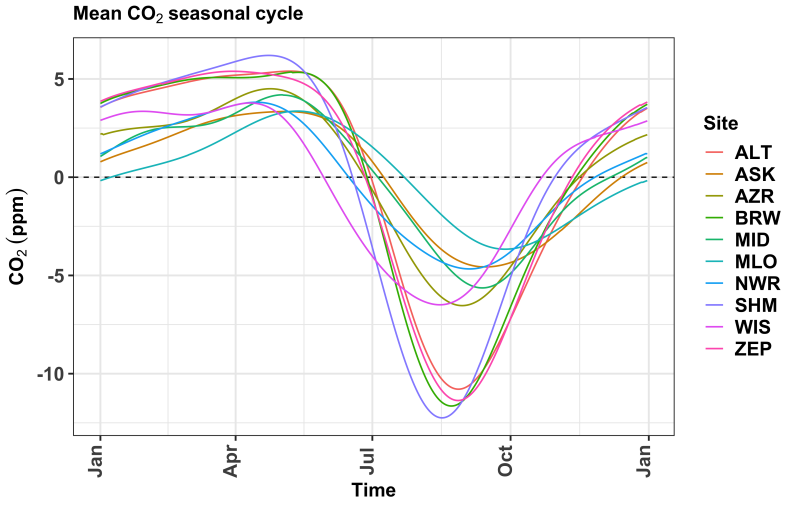

Figure 2. Mean seasonal cycle of CO_2 at studied stations.

3 Method

3.1 Curve fitting and ensemble generation

The time series of CO_2 can be described as the superposition of different modes of variability, acting at different frequencies. A standard approach to extract these modes of variability from the observations ($X_{obs}(t)$) is to define:

$$X_{\text{obs}}(t) = X_{\text{trend}}(t) + X_{\text{seas}}(t) + R(t) \quad (1)$$

where $X_{trend}(t)$ is the low frequency component of the data, which captures variability on multi-annual time scales; $X_{seas}(t)$ represents the seasonal cycle, which can be expressed in terms of a series of harmonics; and R(t) captures the remaining variability (Cleveland et al., 1990). The data used in this study are provided at approximately weekly time steps and includes gaps, as described above. We fill gaps and estimate daily values by fitting a series of curves described in Eq. (1) and use residual bootstrapping (Kreiss and Lahiri, 2012) to generate an ensemble of 500 fitted curves consistent with the observational data for uncertainty estimation. Figure 3 describes the steps involved in curve-fitting and uncertainty estimation. Each step is described in detail below.

First, we separate the long-term trend and mean seasonal cycles ($X_{trend}(t)$ + $X_{seas}(t)$) with a second-degree polynomial and four harmonic sinusoidal functions respectively (Bacastow et al., 1985). The remaining variability, R(t), is referred to as the residuals, which we verified to not show autocorrelation. We then fit a smooth curve to the residuals using the "loess" (local regression) method, which smooths the data, taking into account the gap-lengths in the data. The "Caret" package (Kuhn, 2020) in R provides a method for optimizing the smoothing parameter for the "loess" regression using a mathematical method called k- fold cross validation. The optimization is based on five repetitions of ten fold (k=10) cross-validation, where the

https://doi.org/10.5194/amt-2022-179
Preprint. Discussion started: 27 June 2022

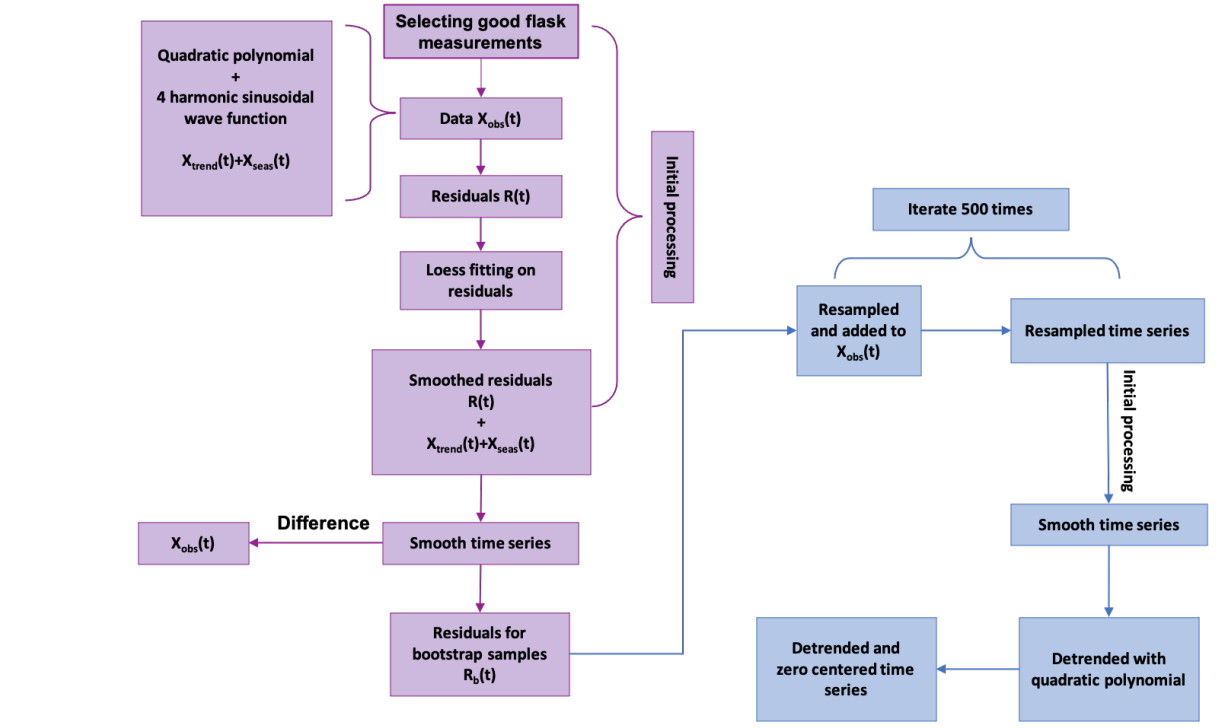

Figure 3. Flow diagram explaining the processes of curve fitting (purple boxes) and ensemble generation (blue boxes).

sub-samples are randomly sampled with restitution. The optimized smoothing parameters are then used to fit a smooth curve to the residuals (R(t)). The resulting smoothed residuals ($R_s(t)$), which contain the remaining variability, are added back to the other components ($X_{trend}(t) + X_{seas}(t)$). This produces a continuous and smooth data set that preserves short-term variations.

Next, we calculate the difference between the smoothed data and the observational data which gives the new set of residuals for generating bootstrap samples ($R_b(t)$). These residuals ($R_b(t)$) are resampled (with replacement) and added to the observational data, producing a resampled time series. The resampled time series is processed as described in the preceding paragraph to obtain a continuous and smooth data set with daily values. From this smoothed time series, a quadratic polynomial is subtracted to remove the long-term trend, resulting in a de-trended, zero-centered time series. The residual resampling and further processing are iterated 500 times to create an ensemble of 500 slightly different de-trended time series (bootstrap samples) which are all consistent with the observations. The classical bootstrapping method (where the observations are resampled) cannot be applied directly to a time series data as the resampling step fails to replicate the time-dependent structure. Hence, we use residual bootstrapping where bootstrapping is applied to the residuals obtained from fitting a model to the raw data. The resampled time series thus show the same time dependence as the observational data, but are produced from the fitted curve and a random component from the residual resampling.

https://doi.org/10.5194/amt-2022-179
Preprint. Discussion started: 27 June 2022


Atmospheric Measurement Techniques Discussions

The ensemble of fitted curves is used to constrain the uncertainty in seasonal cycle metrics estimates. If the estimated metrics differ largely across the bootstrap samples it indicates that the metric estimate is influenced by the inherent uncertainty in extracting a definitive seasonal cycle, by curve fitting the discrete data. Hence, interpreting these metrics without accounting for this uncertainty can be misleading.

3.2 First-derivative threshold method for estimating the timing and duration of the CUP

At high-latitude measuring stations the CUP extends from the seasonal cycle maximum in spring to the seasonal cycle minimum in late summer (Barichivich et al., 2012), driven by CO_2 uptake by ecosystems in the Northern Hemisphere. There is large uncertainty in associating the seasonal cycle maximum with the onset of the CUP, and the definition of the maximum is very sensitive to the curve-fitting method (Barichivich et al., 2012). The uncertainty in associating the timing of a maximum to the start of the CUP is larger than associating it with the zero-crossing dates, especially if the seasonal cycle is characterized by a fairly flat peak, or multiple peaks during the winter (Piao et al., 2008). Hence, previous studies have used the zero-crossing dates and their difference as proxies for the onset, termination and duration of the CUP, respectively. However, the period between the zero-crossing dates includes the CO_2 release period that does not directly affect the CUP (Fig. 1). Therefore, we propose an alternate method to determine the timing and duration of the CUP from data, which more closely corresponds to the spring maximum and the late summer minimum times. This method will be referred to as the first-derivative threshold method (FDT-method). Finally, we estimate the uncertainty in the different CUP estimates by using the spread of the ensemble members.

For each ensemble member we calculate the first derivative of the time series as a proxy for the rate of CO_2 uptake or release. The first derivative is at its minimum when CO_2 uptake is most intense and reaches zero at the peak or trough of the seasonal cycle, i.e. when the sign of the integrated large-scale CO_2 flux changes. However, a peak or a trough (as indicated by zero first-derivative Fig. 4) might not correspond to the spring maximum or late summer minimum if the peak is flat or there are multiple peaks in winter. Our aim is to define the timing of the CUP in such a way that it closely corresponds to the timing of the spring maximum and late summer minimum.

To determine the onset and termination of the CUP from CO_2 mole fractions, we define a threshold, analogous to the way the onset and termination of the growing season are determined from measurements of the CO_2 fluxes (Wang et al., 2019). We define the threshold in terms of the first derivative of the CO_2 dry air mole fraction measurements, as the first derivative can be seen as a proxy for the flux (not an exact correspondence, as the seasonal cycle at each site is affected by the atmospheric transport). For the data points before and after the date of the first derivative minimum (i.e. peak uptake), we identify the points when the first-derivative value is below a given threshold (Fig. 4). The threshold is defined as X% of the first derivative minimum and its value is optimized by testing values ranging from 0% to 20%. These dates correspond, therefore, to the onset and termination of the CUP and their difference then represents the duration of the CUP. The value of X is chosen to minimize the threshold value (as the rate of uptake towards the beginning and end of the CUP approaches zero) while keeping the uncertainty

https://doi.org/10.5194/amt-2022-179
Preprint. Discussion started: 27 June 2022

Atmospheric Measurement Techniques Discussions

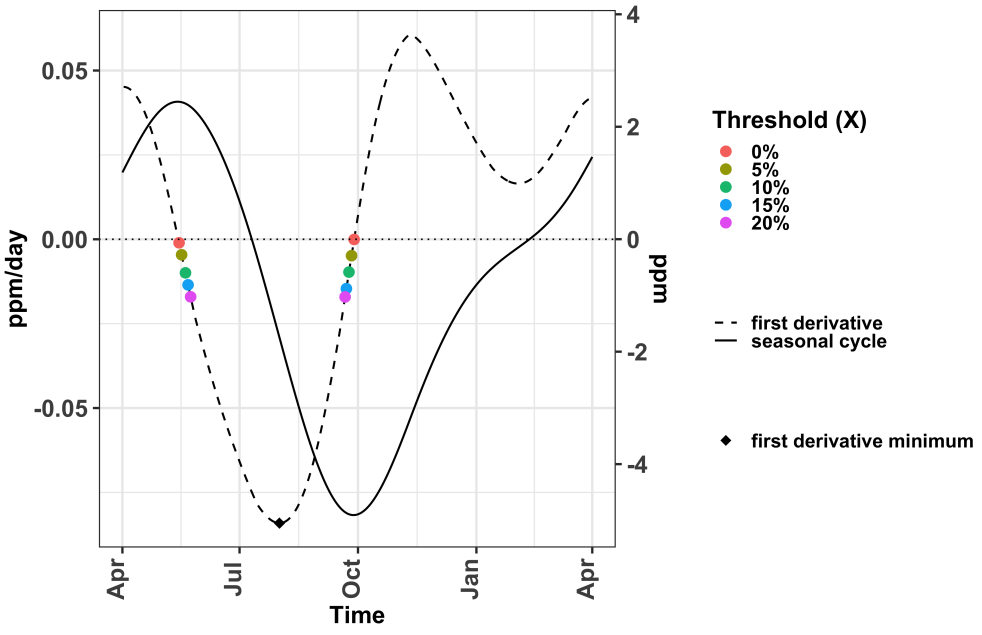

Figure 4. Schematic diagram showing the timing of the CUP as determined by the FDT method. The timing is marked by a threshold, defined in terms of the first derivative of the CO_2 seasonal cycle. It is defined as X% of the first derivative minimum. The value of X is varied from 0% to 20% and the corresponding threshold value is marked on the seasonal cycle first derivative with different colored points. Their timing then defines the timing of the CUP for the different threshold values. The day of the onset and the termination of the CUP are defined by the points before and after the first derivative minimum respectively.

in timing across the ensemble members small.

3.3 CCGCRV fitting and ensemble generation

CCGCRV is a curve fitting method developed by Kirk Thoning and Pieter Tans (Global Monitoring Laboratory (GML), NOAA) in the late 1980s. The method fits a combination of polynomials and annual harmonics to the data to approximate the long-term variation and seasonal cycle. The short-term and interannual variability are retained by filtering the residuals from the fit using a low-pass filter. A detailed description of the routines used for fitting the data and filtering of residual can be found in Thoning et al. (1989). In this study we use the C language version of CCGCRV, freely available at: ftp://ftp.cmdl.noaa.gov/pub/john/ccgcrv/. The values chosen for the input parameters were taken from Table 2 of Pickers and Manning (2015), who optimized them by fitting artificial data (short-term cut-off period f_s: 250 days; long-term cut-off period f_l: 1500 days; number of harmonic terms: 4; degree of polynomial function: 3). Further, we generate 500 bootstrap samples from the CCGCRV-fitted data, producing an ensemble the same size as that derived from the loess-fitted residuals, facilitating the comparison between the two curve-fitting methods. To generate the ensemble members we first apply a CCGCRV fit to

https://doi.org/10.5194/amt-2022-179
Preprint. Discussion started: 27 June 2022


Atmospheric Measurement Techniques Discussions

the data and then resample the residuals from the fit with replacement 500 times. The resampled residuals are added back to the observational data after every resampling event, resulting in 500 resampled time series. Then we apply the CCGCRV fit to every resampled time series creating 500 ensemble members that can be used to quantify the uncertainty in estimated metrics.

4 Results

The seasonal cycles of atmospheric CO_2 based on observational data and the respective ensemble from our curve fitting approach are shown in Fig. 5 for (a) BRW, where the atmospheric mixing ratios have a nearly constant value from January to May followed by a decrease in CO_2 until a minimum is reached in August, and (b) MLO, where the seasonal cycle is characterized by a maximum in May and a minimum in October. It can be noted that the estimated timing of the seasonal cycle maximum varies greatly across the bootstrap samples in BRW (inset of Fig. 5 (a)), where the seasonal cycle is characterized by a flat peak. An earlier peak is likely to be associated with a flat maximum or multiple peaks that may result from transport (Parazoo et al., 2008) or other fluxes, rather than indicating the onset of the uptake period. The timing of the zero-crossing dates at BRW are consistent across the ensemble members, which suggests that the timing of the zero-crossing dates (upward and downward) is less ambiguous. Other higher latitude sites like ALT, SHM and ZEP and lower latitude sites like ASK, WIZ and AZR exhibit similar seasonal cycles, characterized by flat or multiple peaks and less ambiguous zero-crossing dates. However, the zero-crossing dates are closer to the timing of the maximum uptake and release of CO_2 (Manning, 1993) than to the actual onset and termination of the CUP. For example, in Fig. 1, the onset of the CUP occurs in June, however the downward zero-crossing occurs in early July, thus the CUP estimate using the zero-crossing dates explicitly excludes the start of the drawdown period.

At lower latitude stations like MLO, MID and NWR, we find that the zero-crossing dates can vary across ensemble members as shown in Fig. 6 and in such cases the zero-crossing dates are clearly not the best proxy for estimating the duration of the CUP. This is especially the case for the time series at MLO (Fig. 5 (b)), which shows relatively a large spread of 5 days (median of the ensemble spread, rounded to the nearest integer) in the timing of the upward zero-crossing point across the ensemble members. The seasonal cycle at MLO has well-defined peaks and troughs, hence the timings of the seasonal cycle maximum and minimum show only a small spread of 1 day (median of the ensemble spread, rounded to the nearest integer) across the bootstrap samples (inset of Fig. 5 (b)). In this case, the difference between the seasonal cycle maximum and minimum times gives a more robust estimate of the CUP duration.

We estimate the duration of the CUP for each year using different approaches: 1) the difference between the seasonal cycle maximum and minimum times, 2) the difference in the zero-crossing dates and 3) using the proposed FDT method. The three methods are then compared to each other. For the FDT method, we find that the onset of the CUP is best defined when the value of the tuning parameter X is set to 15% and that a value 0% is optimal for defining the termination of the CUP. We optimized the value of the tuning parameter X such that the threshold value remains close to zero while the uncertainty in the estimate of the onset and termination of the CUP is minimized. Increasing the value of X from 15% to 20% results in a similar

https://doi.org/10.5194/amt-2022-179
Preprint. Discussion started: 27 June 2022

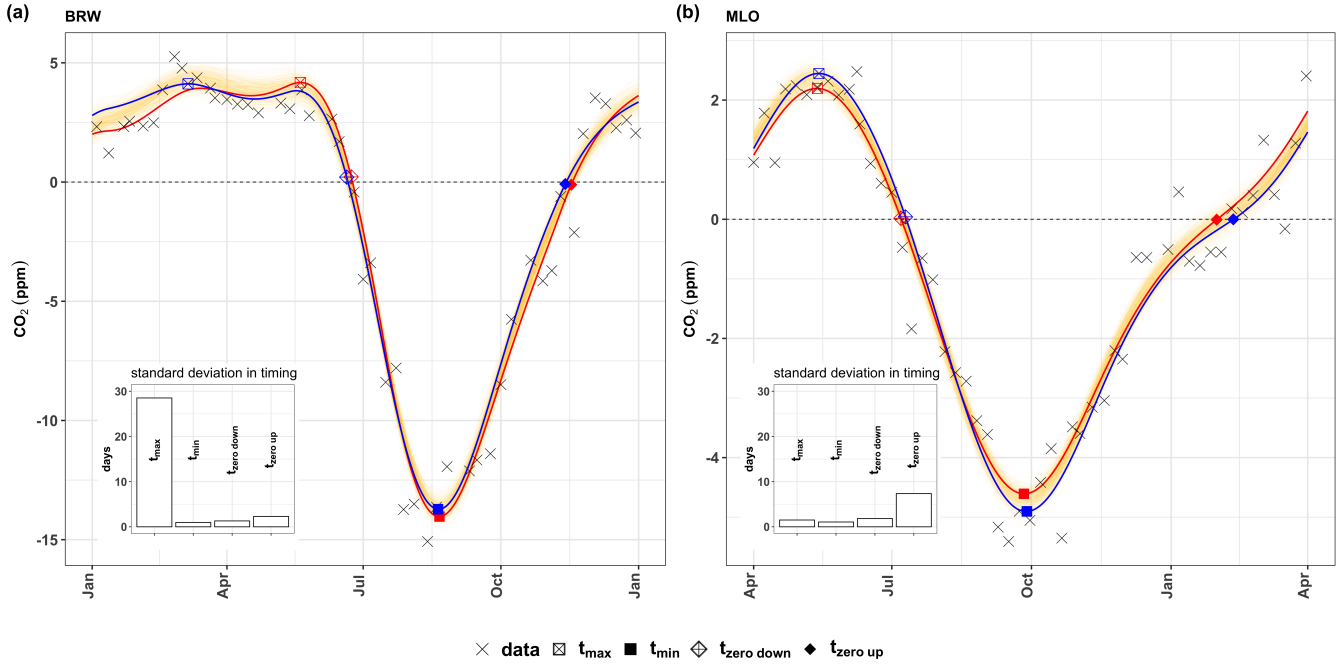

Figure 5. Fitted bootstrap samples (thin yellow lines) representing the seasonal cycle of a year at (a) BRW and (b) MLO. The observational data of the corresponding time period are shown with '×'. Red and blue curves in (a) and (b) highlight two random ensemble members that differ in shape and are marked with the timings of the seasonal cycle maximum (t_{max}), minimum (t_{min}), downward zero-crossing($t_{zero\ down}$) and upward zero-crossing ($t_{zero\ up}$) with the corresponding symbols as in the legend. The vertical bars in the inset show the standard deviation of the labeled metric estimates across the ensemble members.

variability in the estimated onset (Fig. 7) while truncating more of the "actual" CUP. Incidentally, previous studies using flux measurements have also used 15% of the maximum GPP as a threshold to define the start of the growing season (e.g. Wang et al., 2019). Given the robustness of this value, we use 15% as the threshold to define the onset of the CUP. When X is set to 0%, the onset then corresponds to the maximum of the seasonal cycle, hence the large spread in CUP-onset at BRW and ALT, with an interquartile range of 16.5 and 11.5 days respectively, can be attributed to the multiple peaks or broad peak of the CO_2 seasonal cycle at these stations. Compared to the onset, where the data ranges to 35 days (whiskers of the boxplots in Fig.7 (a)), the variability in the termination of the CUP is smaller, with a maximum range of 4.2 days (whiskers of the boxplots in Fig.7 (b)). The standard deviation in the termination is highest at WIS, where the median of the boxplot for different threshold values is within 2.7 ±0.3 days. Hence to define the termination, we chose a threshold such that the standard deviation is minimized at WIS, this is achieved when X is set to 0% (the median of the spread is then 2.4 days).

Figure 8 shows the duration of CUP for all the studied sites, estimated using the three different methods, across the years (median of the 500 ensemble members). The size (interquartile range) of the boxplots varies strongly across the stations for

https://doi.org/10.5194/amt-2022-179
Preprint. Discussion started: 27 June 2022

Atmospheric Measurement Techniques Discussions

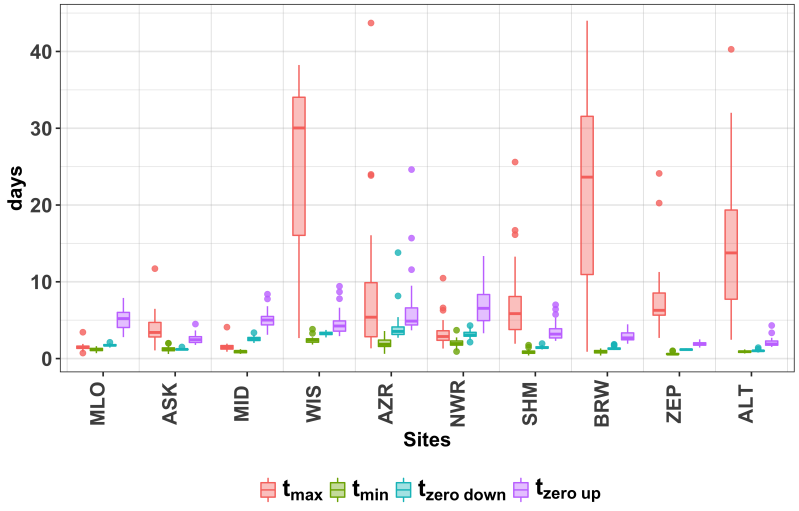

Figure 6. Boxplots showing the bootstrap standard deviation (i.e. the standard error of estimate) in the timing of the seasonal cycle maximum (t_{max}), minimum (t_{min}) and upward ($t_{zero\ up}$), downward ($t_{zero\ down}$) zero crossing dates across the years for loess fitted residual bootstrap samples. The standard deviation in the timing of the different metrics for a year is estimated from the ensemble spread for the year. In the box-plots in this paper, the box denotes the interquartile range (IQR), showing the median with a solid line. The whiskers range from Q_1-1.5x IQR to Q_3+1.5x IQR, where Q_1 and Q_3 are the 25th and 75th percentiles.

CUP duration calculated using the zero-crossing dates and the maxima and minima. At the lower latitude stations MLO, MID and NWR, the variability in the CUP duration is larger than at the other stations when using the zero-crossing dates ("loess zero" in Fig. 8). This is seen in the interquartile range of the "loess zero" boxplots, with values of 43, 35 and 39 days for MLO, MID and NWR respectively, which is larger than for the other stations (within 15 ±5.2 days). The large interquartile range of the CUP-duration estimates using maximum and minimum times at the high latitude sites BRW (51 days) and ALT (35 days) ("loess max.min" in Fig. 8) follows mainly from the large variability in the timing of the seasonal cycle maximum across the ensemble members (Fig. 6).

Using the FDT method proposed in this study, we are able to derive a more robust estimation of the CUP duration across ensemble members (Table 2). Figure 9 compares the standard deviation of the CUP duration across years at all studied sites and methods. The standard deviation is smaller when the FDT method is used for calculating the CUP duration, implying that this metric is better determined. The interquartile range of standard deviation is largest for the method using the dates of the seasonal cycle maximum and minimum, especially at higher latitude stations like BRW (20 days) and ALT (12 days) and lower latitude station like WIS (18 days). This follows from the shape of the seasonal cycle. These results indicate that the duration of the CUP should not be estimated based on the seasonal cycle maximum and minimum at higher latitude stations and other stations where the seasonal cycle has flat or multiple peaks. At MLO, NWR and MID, using the zero-crossing dates to estimate

https://doi.org/10.5194/amt-2022-179
Preprint. Discussion started: 27 June 2022

Atmospheric Measurement Techniques Discussions

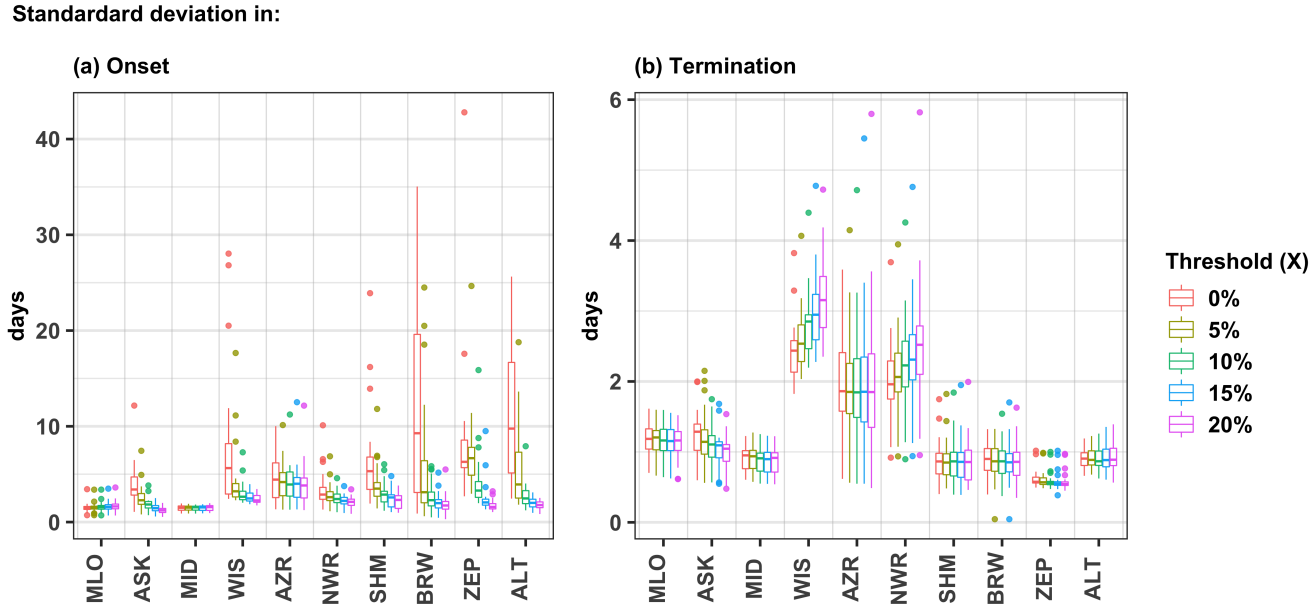

Figure 7. Standard deviation (among ensemble members) in the onset (a) and termination (b) of the CUP across years. Differently colored boxes represents different threshold values. The threshold value with X equal to 15% and 0% is chosen for defining the onset and termination of the CUP respectively, for all the studied sites.

the CUP duration results in a larger standard deviation (median of the spread is 5.7, 5.7 and 7.5 days respectively) in the CUP duration estimates relative to the other methods used (the median of the spread for the other methods is within 2 ±0.6 days), which can be attributed to the change of shape of the seasonal cycle around the upward zero-crossing point (Fig. 1).

In Fig. 10, we show two random ensemble members (red and blue thick lines), one each from two different years from MLO. The two selected years have a similar CUP duration when estimated using the times of the seasonal cycle maximum and minimum (138 days for the red curve and 135 days for the blue). However, the change of shape following the seasonal cycle minimum results in differences in the timing of the upward zero-crossing point for the two years, leading to differing estimates of the CUP duration when using the zero-crossing method for these years (168 days for the red curve and 188 days for the blue). This suggests that the skewness of the seasonal cycle can affect the interpretation of CUP for individual years by causing variability in the timing of the upward zero-crossing across the ensemble members (Fig. 5(b)) as well as between the years (Fig. 10). Hence, an alternative to the timing of the zero-crossing dates is required to robustly estimate the CUP.

Here we show that using the FDT method, the uncertainty in the CUP estimate is reduced across all the studied sites. A previous study that used the zero-crossing dates to estimate the CUP also noted the large uncertainty in using the seasonal

https://doi.org/10.5194/amt-2022-179
Preprint. Discussion started: 27 June 2022

Atmospheric Measurement Techniques Discussions

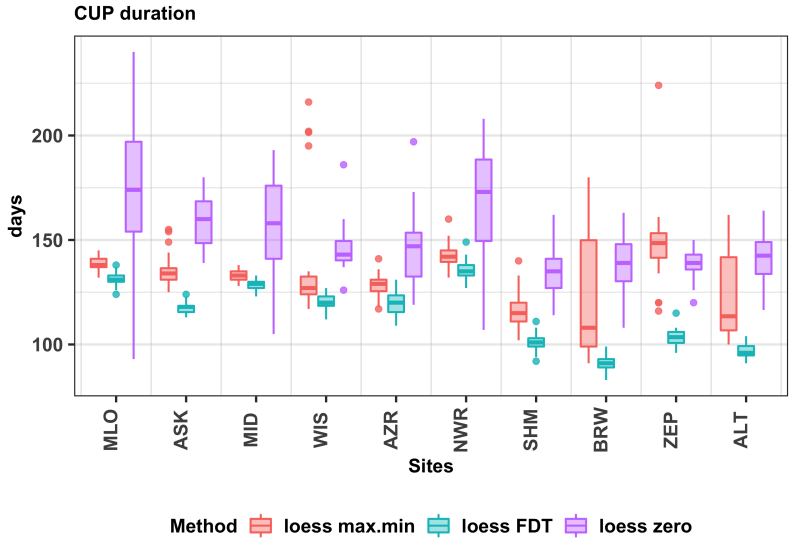

Figure 8. Boxplot showing the distribution of the median CUP duration across all years estimated for the loess-fitted residual bootstrap samples using different methods at the studied sites. The median of the CUP duration for a given year is estimated from the ensemble spread for that year. The CUP duration is calculated using three methods, namely: as the period between the seasonal maximum and minimum (loess max.min), the FDT method (loess FDT), and using the zero-crossing dates (loess zero)).

cycle maximum and minimum (Barichivich et al., 2012), which is similar to our result (Fig. 9). Therefore this method will not be considered in further analysis here.

However, when CUP duration is estimated using the zero-crossing dates there is also large uncertainty at the lower latitude stations (e.g. the interquartile range for the 'loess zero´ boxplot for MLO is 43 days, Fig. 8). This can be attributed to the variability in the skewness of the seasonal cycle at these sites. The FDT method is not affected by this skewness and therefore gives a more robust estimate of the timing and duration of the CUP even at lower latitudes.

To further test the robustness of the CUP estimates based on the loess-fitted residual bootstrap method, we compared them against the CUP estimates from an ensemble using the CCGCRV curve-fitting method. Comparable results were obtained when the same CUP estimation method (zero-crossing dates / FDT method) was applied to the ensemble members using two different curve-fitting methods (Fig. 11). The CUP duration calculated from the CCGCRV ensemble using the zero-crossing dates and the FDT method were within the range of their corresponding estimates from the loess-fitted ensemble members. The mean difference between the median of the "CCG zero" and "loess zero" estimates in Fig. 11 is 2.3 days, and between the median of "CCG FDT" and "loess FDT" estimates the mean difference is only 0.7. Furthermore, we show that for both

https://doi.org/10.5194/amt-2022-179
Preprint. Discussion started: 27 June 2022

Atmospheric Measurement Techniques Discussions

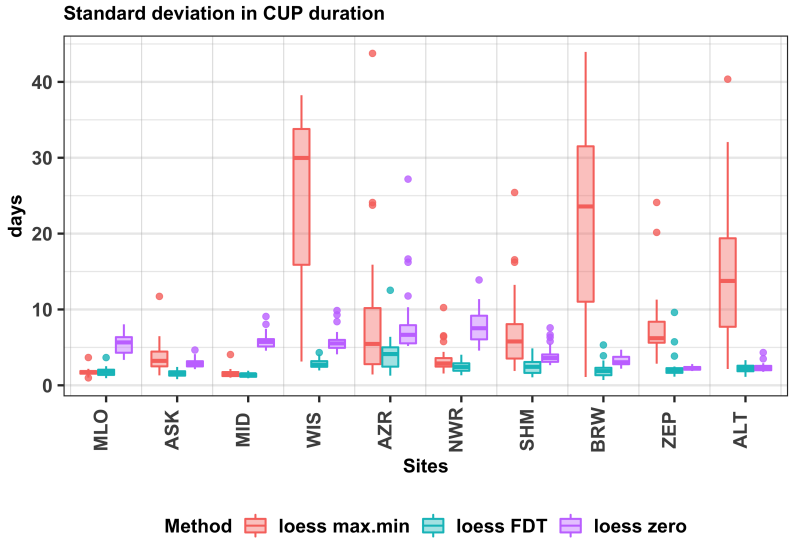

Figure 9. Boxplot showing the distribution of the standard deviation in CUP duration across all years estimated from the loess-fitted residual bootstrap samples using different methods at the studied sites. The standard deviation in CUP duration for a given year is estimated from the ensemble spread for that year. The CUP duration is calculated using three methods as described by the legend (and as in Figure 8).

curve-fitting methods the standard deviation in the CUP duration estimate across the ensemble members is lowest for the FDT method (Fig. 12). Thus, the FDT method produces robust results irrespective of the particular curve fitting method.

5 Discussion

This study introduces a novel method for quantifying the uncertainty in the CO_2 seasonal cycle curve fitting by creating multiple residual bootstrap samples. The spread of this ensemble provides a measure of the uncertainty in the estimation of seasonal cycle metrics. The ensemble members are consistent with the observational data; hence we consider the variability of the metric estimate across the ensemble as a measure of uncertainty.

The shape of the CO_2 seasonal cycle varies with latitude. For example, the seasonal cycle at MLO has clearly defined peaks while at BRW there is a nearly flat peak followed by a decrease in CO_2 levels during a short time when the vegetation at high latitudes actively photosynthesizes (Cleveland et al., 1983). If the seasonal cycle were determined solely by the biospheric fluxes then the onset and termination of the CUP would be marked by the timing of the seasonal cycle maximum and minimum respectively (Barichivich et al., 2012). However at the higher latitude stations the seasonal cycle has a broader peak or multiple peaks in winter and the timing of the seasonal cycle maximum cannot be interpreted as the onset of the CUP. Further, our analysis shows that there is large uncertainty in the timing of the seasonal cycle maximum (Fig. 6) at higher latitude stations which is in agreement with previous studies (e.g. Barichivich et al., 2012; Piao et al., 2008), that have used the timing of the

https://doi.org/10.5194/amt-2022-179
Preprint. Discussion started: 27 June 2022

Atmospheric Measurement Techniques Discussions

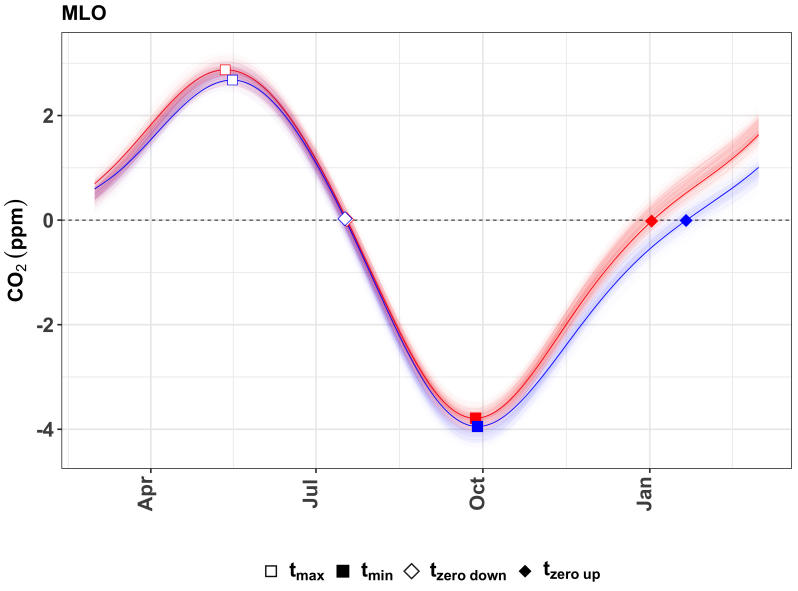

Figure 10. Bootstrap samples representing the seasonal cycle of two different years (red and blue) with similar time periods between the seasonal cycle maximum and minimum. Thin red and blue lines represent the ensemble spread for the two years. The thicker red/blue lines represent a random ensemble member from each year and these are marked with the timings of the seasonal cycle maximum, minimum and zero-crossing dates as described in the legend.

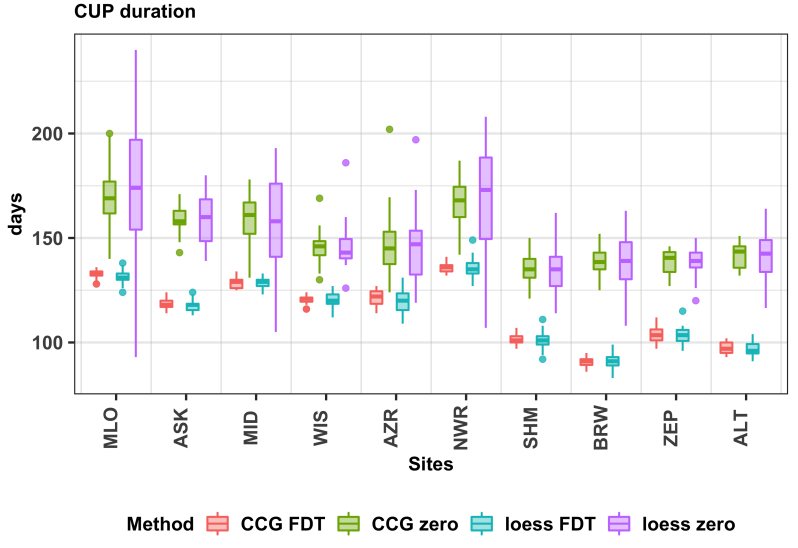

Figure 11. Boxplot showing the distribution of the median of the CUP duration across years (as described in Fig. 8), estimated for the CCGCRV-fitted residual bootstrap samples using the FDT method (CCG FDT, red), the zero-crossing dates (CCG zero, green), and for the loess-fitted residual bootstrap samples using the FDT method (loess FDT, blue) and the zero-crossing dates (loess zero, purple).

https://doi.org/10.5194/amt-2022-179
Preprint. Discussion started: 27 June 2022

Atmospheric Measurement Techniques Discussions

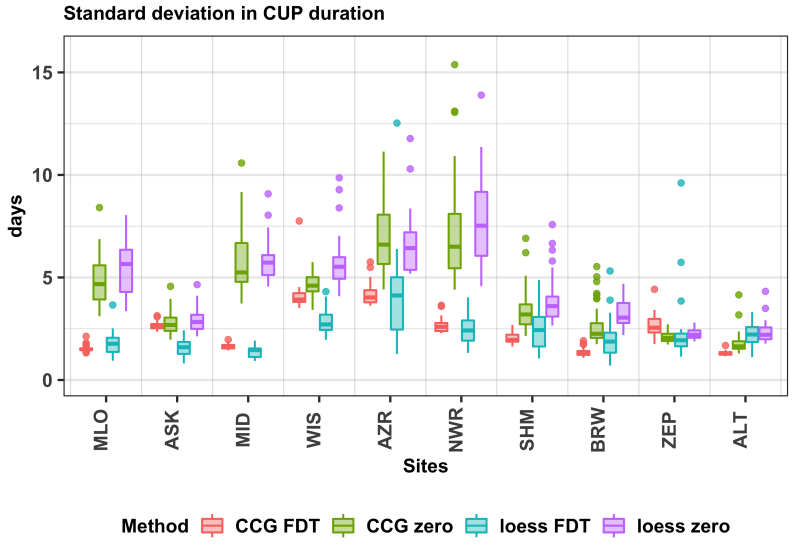

Figure 12. Boxplot showing the distribution of the standard deviation in the CUP duration across years (as described in Fig. 8), estimated for the CCGCRV-fitted residual bootstrap samples using the FDT method (CCG FDT, red), the zero-crossing dates (CCG zero, green), and for the loess-fitted residual bootstrap samples using the FDT method (loess FDT, blue) and the zero-crossing dates (loess zero, purple). Note that six outliers (with values between 16 to 30 days) corresponding to AZR has been removed for ease of visualization.

zero-crossing dates as an alternative to define the CUP. We find this approach to be less ambiguous for sites where the seasonal cycle peaks are not clearly defined (Fig. 6).

However, at MLO, MID and NWR (Fig. 9), the standard deviation in the estimated CUP duration is the largest when estimated using the zero-crossing dates relative to the other methods of estimation. For these sites (MLO, MID and NWR) the timing of the upward zero-crossing date is less certain, with a higher standard deviation relative to the other metrics shown in Fig. 6. The seasonal cycle at these sites is characterized by clearly defined peaks, hence there is less uncertainty in the timing of the seasonal cycle maximum and minimum (i.e. smaller standard deviation relative to the other metrics shown in Fig. 6). At such sites the period between seasonal cycle maxima and minima gives a better representation of the CUP duration than the period between the zero-crossing dates.

The time period between the zero-crossing dates includes parts of both the CO_2 uptake and release period. However, the CUP is defined as the period when the CO_2 uptake is greater than the CO_2 release. Changes in CO_2 release after the upward zero-crossing do not directly affect the true CUP duration, unlike the timing of the minimum, which is more crucial in defining the CUP duration. However, the maximum CO_2 uptake occurs within the CUP, hence any change in the maximum uptake (timing and rate) influences the CUP duration more directly. The FDT method we propose for estimating the timing and duration

https://doi.org/10.5194/amt-2022-179
Preprint. Discussion started: 27 June 2022

Atmospheric Measurement Techniques Discussions

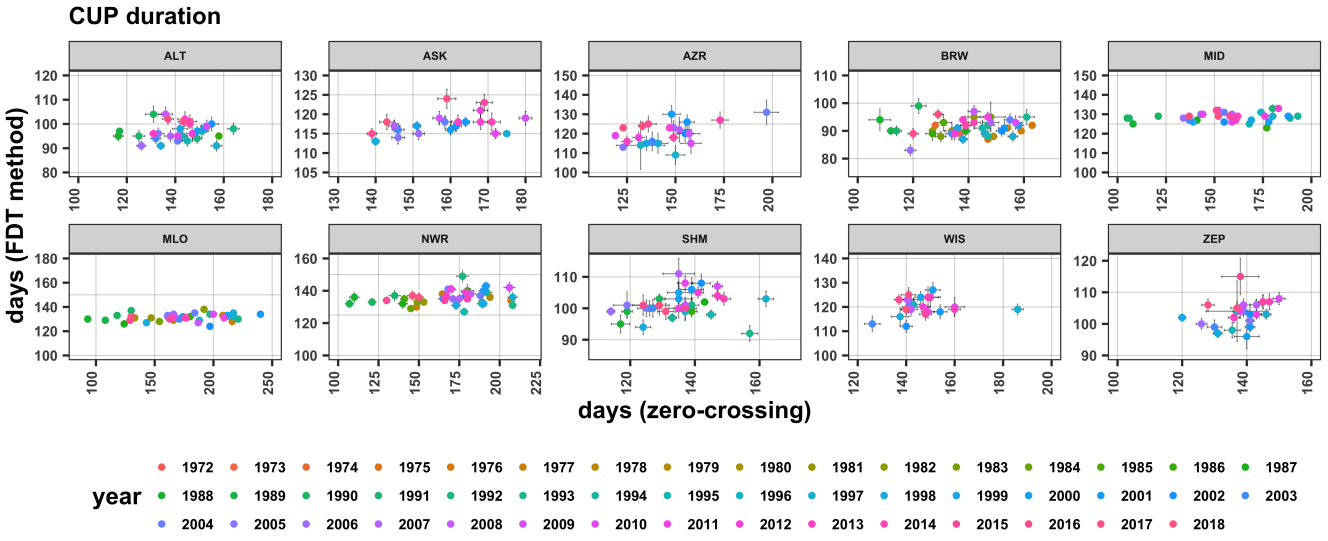

Figure 13. CUP duration estimated from the loess-fitted residual bootstrap samples using the timing of the zero-crossing dates (x-axis) against that estimated using the FDT method (y-axis) for different sites (panels). The colored points show estimates for different years and the associated error bars show the spread (median ±sd) of the ensemble.

of the CUP directly depends on the maximum CO_2 uptake (timing and rate) and thus is more closely related to the actual CUP.

Using the first derivative threshold method to define the onset and termination of the CUP, we are able to reduce the spread among ensemble members when calculating the timing and duration of the CUP. We find that by using this method, the variability among ensemble members is reduced in comparison to using the zero-crossing dates to estimate the CUP duration. The difference between the CUP estimates using the two different methods varies from year to year, suggesting that the estimates using zero-crossing dates cannot be corrected by simply adding an offset, as can be seen in Fig. 13.

We also tested the different methods for CUP estimation on ensembles created using a different curve-fitting approaches, to compare the proposed curve-fitting method to a well established method. The CUP estimates from ensemble members of both curve-fitting methods produced comparable results when the same CUP estimation method was applied, which shows that the proposed curve-fitting method is robust. The CUP duration estimated using the zero-crossing dates shows larger spread for sites like MLO (with an interquartile range of 16 days for CCGCRV fitted data and 43 days for loess fitted data) irrespective

https://doi.org/10.5194/amt-2022-179
Preprint. Discussion started: 27 June 2022


Atmospheric Measurement Techniques Discussions

of the curve-fitting method used. This is attributed to variability in the upward zero-crossing dates due to the skewness of the seasonal cycle during periods of net release and is similar in both the curve fitting methods. Furthermore, we find that using the FDT method of CUP estimation resulted in smaller spread across the bootstrap samples for both the curve-fitting methods (Fig. 12). This suggests that the period within the onset and termination defined by the FDT method, which includes only part of the drawdown period, is less variable than the time period between the zero-crossing dates, which includes parts of both the drawdown and release periods. Here we have shown how this approach can be used to improve estimate of the CUP. This could be extended to improve estimates of other metrics.

The approach presented here could be performed on hourly or daily in-situ data, which are accepted as representing background conditions. However, there is considerable auto-correlation between consecutive days in daily measurements which reduces the degrees of freedom of variability. This limits the number of independent events to five or six per month, which is comparable to the scale of our weekly measurements. It is recommend that before applying this approach to in-situ data, a comparison on the number of registered independent events for selected sites be made (gml.noaa.gov).

In this study we show that CO_2 seasonal cycle metric estimates can be strongly sensitive to the method used, hence any method must be thoroughly evaluated before it can be used to draw conclusions from the data. The metric estimate across the ensemble members provides an uncertainty range, hence allowing to evaluate the robustness of estimated values. Here this approach was used to test a novel method against an existing method for estimating the timing and duration of the CUP. In a similar fashion, this could be used to evaluate a newly proposed method or select an optimal method for evaluating any other metric.

6 Conclusions

We propose a method for estimating the timing and duration of the CUP from a discrete time series of CO_2 dry air mole fraction data. The uncertainty in the metric estimate is quantified using an ensemble of fitted time series generated through residual bootstrap sampling. Previous studies have used the timing of the zero-crossing dates as a proxy for defining the CUP, however we find that the timing of the upward zero-crossing point is influenced by the shape of the seasonal cycle, leading to large variability in the estimated CUP duration across the ensemble members for a given year for some of the studied sites, particularly at lower latitudes. The variability in the CUP duration across the ensemble members for a given year is lower (for all the studied sites) when it is calculated using the FDT method. The FDT method depends directly on the timing and rate of the maximum CO_2 uptake; hence the method is not affected by the shape change of the seasonal cycle outside the time period during which the CO_2 uptake is larger than the CO_2 release. To test the impact of the curve-fitting method used, we generated bootstrap samples using both loess-fitted residuals and CCGCRV. The CUP duration estimated using the FDT method results in smaller spread for both curve-fitting methods. Further, for both curve-fitting methods, the standard deviation in the estimates across the ensemble members is smaller when using the FDT method, suggesting that the FDT method gives robust estimates.

https://doi.org/10.5194/amt-2022-179
Preprint. Discussion started: 27 June 2022


Atmospheric Measurement Techniques Discussions

Thus, the FDT method allows for a robust estimate of the CUP that better reflects the CO_2 drawdown period. Here, estimates from multiple bootstrap samples were used to estimate the uncertainty in the estimate of the CUP onset and duration. This approach could be extended to other metrics of seasonal cycle analysis or to other curve-fitting methods, as was shown with the comparison to the CCGCRV results.

Data availability. The CO_2 dry air mole fraction data for ALT, BRW and MLO is available from (Dlugokencky et al., 2019) and for the other stations used in this study from (Dlugokencky et al., 2020).

Author contributions. The coding and analysis was performed by TK with contributions of MR. The study was conceptualised by JM, AB and MR with contributions from WP. JM, AB, WP, MR and PT contributed with expert knowledge.The original manuscript was drafted by TK which was reviewed and edited by WP, JM, AB, MR and PT.

Competing interests. The authors declare that they have no conflict of interest.

https://doi.org/10.5194/amt-2022-179
Preprint. Discussion started: 27 June 2022

Atmospheric Measurement Techniques Discussions

Table 2. The inter-quartile range of the standard deviation in the CUP duration across all years as described in Fig. 9, rounded to the nearest integer (day). Values are given for three different method of estimation for each site.

Sites	Time period	sd CUP duration (days)	Method
MLO	1977-2017	4-7	zero
		1-2	max.min
		1-2	FDT method
ASK	1996-2018	2-4	zero
		2-5	max.min
		1-2	FDT method
MID	1986-2018	5-7	zero
		1-2	max.min
		1-2	FDT method
WIS	1996-2018	5-8	zero
		12-37	max.min
		2-4	FDT method
AZR	1996-2018	5-15	zero
		2-22	max.min
		2-6	FDT method
NWR	1976-2018	5-10	zero
		2-4	max.min
		2-3	FDT method
SHM	1986-2018	3-6	zero
		3-13	max.min
		1-4	FDT method
BRW	1972-2017	3-4	zero
		2-37	max.min
		1-3	FDT method
ZEP	1995-2018	2-3	zero
		5-11	max.min
		1-3	FDT method
ALT	1986-2017	2-3	zero
		3-24	max.min
		1-3	FDT method

https://doi.org/10.5194/amt-2022-179
Preprint. Discussion started: 27 June 2022


Atmospheric Measurement Techniques Discussions

References

Bacastow, R. B., Keeling, C. D., and Whorf, T. P.: Seasonal amplitude increase in atmospheric CO2 concentration at Mauna Loa, Hawaii, 1959–1982, Journal of Geophysical Research: Atmospheres, 90, 10 529–10 540, https://doi.org/https://doi.org/10.1029/JD090iD06p10529, 1985.

Barichivich, J., Briffa, K., Osborn, T., Melvin, T., and Caesar, J.: Thermal growing season and timing of biospheric carbon uptake across the Northern Hemisphere, Global Biogeochemical Cycles, 26, 4015–, https://doi.org/10.1029/2012GB004312, 2012.

Barlow, J. M., Palmer, P. I., and Bruhwiler, L. M.: Increasing boreal wetland emissions inferred from reductions in atmospheric CH_4 seasonal cycle, Atmospheric Chemistry and Physics Discussions, 2016, 1–38, https://doi.org/10.5194/acp-2016-752, 2016.

Chan, Y. H. and Wong, C. S.: Long-term changes in amplitudes of atmospheric CO2 concentrations at Ocean Station P and Alert, Canada, Tellus B, 42, 330–341, https://doi.org/https://doi.org/10.1034/j.1600-0889.1990.t01-4-00003.x, 1990.

Cleveland, R. B., Cleveland, W. S., McRae, J. E., and Terpenning, I.: STL: A Seasonal-Trend Decomposition Procedure Based on Loess (with Discussion), Journal of Official Statistics, 6, 3–73, 1990.

Cleveland, W. S., Freeny, A. E., and Graedel, T. E.: The seasonal component of atmospheric CO2: Information from new approaches to the decomposition of seasonal time series, Journal of Geophysical Research: Oceans, 88, 10 934–10 946, https://doi.org/https://doi.org/10.1029/JC088iC15p10934, 1983.

Dlugokencky, E., Mund, J. W., Crotwell, A. M. andCrotwell, M. J., and Thoning, K. W.: Atmospheric Carbon Dioxide Dry Air Mole Fractions from the NOAA GML Carbon Cycle Cooperative Global Air Sampling Network, 1968-2018, Version: 2019-07, https://doi.org/https://doi.org/10.15138/wkgj-f215, 2019.

Dlugokencky, E., Mund, J. W., Crotwell, A. M. andCrotwell, M. J., and Thoning, K. W.: Atmospheric Carbon Dioxide Dry Air Mole Fractions from the NOAA GML Carbon Cycle Cooperative Global Air Sampling Network, 1968-2019, Version: 2020-07, https://doi.org/https://doi.org/10.15138/wkgj-f215, 2020.

gml.noaa.gov: Trends in CO2, [online] Available from:https://gml.noaa.gov/ccgg/trends/, accessed: 2022-06-8.

Keeling, C. D.: The Concentration and Isotopic Abundances of Carbon Dioxide in the Atmosphere, Tellus, 12, 200–203, https://doi.org/https://doi.org/10.1111/j.2153-3490.1960.tb01300.x, 1960.

Keeling, C. D., Chin, J. F. S., and Whorf, T. P.: Increased activity of northern vegetation inferred from atmospheric CO2 measurements, Nature, 382, 146–149, 1996.

Keeling, R. F., Graven, H. D., Welp, L. R., Resplandy, L., Bi, J., Piper, S. C., Sun, Y., Bollenbacher, A., and Meijer, H. A. J.: Atmospheric evidence for a global secular increase in carbon isotopic discrimination of land photosynthesis, Proceedings of the National Academy of Sciences, 114, 10 361–10 366, https://doi.org/10.1073/pnas.1619240114, 2017.

Kreiss, J.-P. and Lahiri, S. N.: 1 - Bootstrap Methods for Time Series, in: Time Series Analysis: Methods and Applications, edited by Subba Rao, T., Subba Rao, S., and Rao, C., vol. 30 of *Handbook of Statistics*, pp. 3–26, Elsevier, https://doi.org/https://doi.org/10.1016/B978-0-444-53858-1.00001-6, 2012.

Kuhn, M.: caret: Classification and Regression Training, https://CRAN.R-project.org/package=caret, r package version 6.0-85, 2020.

Langenfelds, R. L., Francey, R. J., Pak, B. C., Steele, L. P., Lloyd, J., Trudinger, C. M., and Allison, C. E.: Interannual growth rate variations of atmospheric CO2 and its δ13C, H2, CH4, and CO between 1992 and 1999 linked to biomass burning, Global Biogeochemical Cycles, 16, 21–1–21–22, https://doi.org/https://doi.org/10.1029/2001GB001466, 2002.

https://doi.org/10.5194/amt-2022-179
Preprint. Discussion started: 27 June 2022

Manning, M. R.: Seasonal Cycles in Atmospheric CO2 Concentrations, in: The Global Carbon Cycle, edited by Heimann, M., pp. 65–94, Springer Berlin Heidelberg, Berlin, Heidelberg, 1993.

Nakazawa, T., Ishizawa, M., Higuchi, K., and Trivett, N. B. A.: Two curve fitting methods applied to co2 flask data, Environmetrics, 8, 197–218, https://doi.org/https://doi.org/10.1002/(SICI)1099-095X(199705)8:3<197::AID-ENV248>3.0.CO;2-C, 1997.

Parazoo, N. C., Denning, A. S., Kawa, S. R., Corbin, K. D., Lokupitiya, R. S., and Baker, I. T.: Mechanisms for synoptic variations of atmospheric CO_2 in North America, South America and Europe, Atmospheric Chemistry and Physics, 8, 7239–7254, https://doi.org/10.5194/acp-8-7239-2008, 2008.

Park, T., Chen, C., Macias-Fauria, M., Tømmervik, H., Choi, S., Winkler, A., Bhatt, U. S., Walker, D. A., Piao, S., Brovkin, V., Nemani, R. R., and Myneni, R. B.: Changes in timing of seasonal peak photosynthetic activity in northern ecosystems, Global Change Biology, 25, 2382–2395, https://doi.org/https://doi.org/10.1111/gcb.14638, 2019.

Piao, S., Ciais, P., Friedlingstein, P., Peylin, P., Reichstein, M., Luyssaert, S., Margolis, H., Fang, J., Barr, A., Chen, A., Grelle, A., Hollinger, D., Laurila, T., Lindroth, A., Richardson, A., and Vesala, T.: Net carbon dioxide losses of northern ecosystems in response to autumn warming, Nature, 451, 49–52, https://doi.org/10.1038/nature06444, 2008.

Piao, S., Liu, Z., Wang, Y., Ciais, P., Yao, Y., Peng, S., Chevallier, F., Friedlingstein, P., Janssens, I. A., Peñuelas, J., Sitch, S., and Wang, T.: On the causes of trends in the seasonal amplitude of atmospheric CO2, Global Change Biology, 24, 608–616, https://doi.org/https://doi.org/10.1111/gcb.13909, 2018.

Pickers, P. A. and Manning, A. C.: Investigating bias in the application of curve fitting programs to atmospheric time series, Atmospheric Measurement Techniques, 8, 1469–1489, https://doi.org/10.5194/amt-8-1469-2015, 2015.

Tans, P. P. K. W. T., Elliott, W., and Conway, T. J.: Background Atmospheric CO2 patterns from weekly flask samples at Barrow, Alaska: Optimal signal recovery and error estimates, in The Statistical Treatment of CO2 Data Records, NOAA Technical Memorandum, 173,131, 112–123, 1989.

Thoning, K. W., Tans, P. P., and Komhyr, W. D.: Atmospheric carbon dioxide at Mauna Loa Observatory: 2. Analysis of the NOAA GMCC data, 1974–1985, Journal of Geophysical Research: Atmospheres, 94, 8549–8565, https://doi.org/https://doi.org/10.1029/JD094iD06p08549, 1989.

Trivett, N. B. A., K, H., and S., S.: Trends and seasonal cycles of atmospheric CO2 over Alert, Sable Island, and Cape St. James, as analyzed by forward stepwise regression technique, NOAA Technical Memorandum ERL ARL- 173, Air Resources Laboratory, Silver Spring, Maryland, USA, 173,131, 27–42, 1989.

Wang, X., Xiao, J., Li, X., Cheng, G., Ma, M., Zhu, G., Altaf Arain, M., Andrew Black, T., and Jassal, R. S.: No trends in spring and autumn phenology during the global warming hiatus, Nature Communications, 10, 2389, https://doi.org/10.1038/s41467-019-10235-8, 2019.